



Immobilization of Synthesized TiO₂ Nano-sheets onto the Surface of the Mesh and its Modification Effect on the Wettability Behavior

Landry Biyoghe Bi Ndong^{1,3,*}, Frank Herve Yeo Kanfola¹, Bo Bai², Hui Huang³ and Chi He⁴

¹College of Environmental Science and Engineering, Chang'an University, Xi'an, 710054, P.R China

²Qinghai Provincial Key Laboratory of Tibetan Medicine Research, Xining, 810001, P.R China

³Petroleum Exploration and Production Research Institute, Sinopec, Beijing 100083, P.R China

⁴State Key Laboratory of Multiphase Flow in Power Engineering, School of Energy and Power Engineering, Xi'an Jiaotong University, Xi'an 710049, PR China

ABSTRACT

In this study, a widely used TiO₂ was synthesized by a simple hydrothermal solution and characterized by using X-ray diffraction, scanning electron microscopy and energy dispersive spectroscopy. Analysis results showed that the synthesized TiO₂ was in anatase form and consisted of well-defined sheet-shaped structures having a rectangular outline. Moreover, the calcination temperature remarkably affected the crystalline phase of the product as a mixture of rutile and anatase phase was obtained with the product calcinated at 1000°C. The synthesized TiO₂ was further involved in a coated process using stainless mesh as a substrate. The contact angle measurement revealed a modification on the surface wettability of the mesh with the underwater oil contact angle larger than 150° and the oil/water separation efficiency over 90% even after thirty cycles of reuses. The substrate analysis indicated that the TiO₂ made a separating layer thus, affected the wettability behavior of the mesh. The present study suggested the effectiveness of immobilizing synthesized TiO₂ for the modification of surface wettability.

Keywords: TiO₂ nano-sheets; Membrane coating technology; Surface wettability; Oil/water separation

INTRODUCTION

Titanium dioxide (TiO₂), wide band gap energy semiconductor (3.02 eV), has been largely investigated since Fujishima and Honda [1-4] discovered the photocatalytic of water splitting on TiO₂ electrodes. Owing to its nontoxicity, biological and chemical inertness, strong oxidizing power, and long-term stability against corrosion, TiO₂ photo-catalyst has been intensively used in decontamination, purification, and/or deodorization of air as well as polluted water [5-7]. In fact, the irradiation of aqueous TiO₂ suspensions at wavelengths that is shorter than the band gap ($\lambda < 410$ nm) result in electron-hole pair generation. These pairs eventually migrate to the surface of TiO₂ to be involved in a series of redox reactions. The electrons reduce Ti (IV) into Ti (III) and subsequently react with the absorbed oxygen (O₂) on TiO₂ surface to superoxide radical anions (O₂^{•-}). At the same time, the hole (h⁺) reacts with the absorbed water molecules (H₂O) to generate hydroxyl radicals (OH[•]) [8-10]. In that way, Biyoghe et al.

reported the synthesized and the application of TiO₂ for dechlorination of harmful and environmental persistence tetrachloroethene (PCE), trichloroethene (TCE) and 1,1,1-trichloroethane (TCA) in the aqueous phase [6].

Unfortunately, TiO₂ powder suffers for the difficulty to separate it from treated water that limits its industrial application. To overcome that problem, the literature review reported some studies on the immobilization of TiO₂ powder onto substrates [11-14]. Especially in oil/water separation process, the immobilization of TiO₂ powder onto the surface of the filter could modify its wettability and such materials have been intensively studied in various fields [15-18]. Such modified substrates which simultaneously display superhydrophilic and underwater superoleophobic properties with water contact angle (Wca) less than 5° an oil contact angle (Oca) greater than 150°, are more desirable over traditional hydrophilic and oleophobic materials that they allow water to pass while simultaneously repelling oil on their surface, thus effectively avoids the possibility of membrane clogging by the viscous oil [19-22].

It is as been demonstrating that the hydrophilicity of the substrate depends on the presence of the hydroxyl group (OH-) on its surface [23-28]. High is the concentration of the hydroxyl group (OH-), strong is the hydrophilicity of the substrate. So, due to its strong oxidizing power, the substrate coated with TiO₂ can highly generate hydroxyl radical in heterogeneous solution, that increase the hydrophilicity of the surface and resulting in high oil repellency properties and thus, limiting the fouling of the membrane by viscous oil [20,23,29,30].

In the present study, we investigate the applicability of our previous synthesized TiO₂ nano-sheets on the surface mesh coating. TiO₂ nano-sheets were synthesized by a simple hydrothermal method using tetrabutyl titanate and hydrofluoric acid. Following calcination at 450, 550, 600, 700 and 1000°C, respectively, the synthesized TiO₂ was characterized by X-ray diffraction (XRD), scanning electron microscopy (SEM) and energy dispersive spectroscopy (EDS). The immobilization on the surface of the available stainless mesh was performed using a dip coating process with dimethyl sulfoxide (DMSO) as a solvent. The modified mesh was involved in oil/water separation operation and further characterized by XRD, and SEM and EDS analyses. It is expected that the results of this study can contribute to the ongoing research on the wide industrial application of TiO₂ powder.

MATERIALS AND METHODS

Chemicals

Tetrabutyl-titanate (Ti (OBu)₄, 98%), hydrofluoric acid (HF, 45%), ethanol (99%), dimethyl sulfoxide (DMSO, 99%), acetone (99%) and petroleum ether were purchased from Sinopharm Chemical Reagent Beijing Co., Ltd. (Beijing, China), stainless steel mesh with pore size of 75 μm was provided from Beijing University first affiliated material laboratory (Beijing, China), leybonol and olive oil were purchased from local oil station and shop, respectively. All chemicals were of analytical grade and used without further purification. Ultrapure water from a Milli-Q water process (Classic DI, ELGA, Marlow, U.K.) was used in all experiments.

Catalysts Preparation

TiO₂ anatase nano-sheets were synthesized according to previous hydrothermal method [31]. Briefly, 30 mL Ti(OBu)₄ and 2 mL HF were mixed in a dried Teflon autoclave with a capacity of 50 mL and then kept at 180°C for 24 h. After cooling to room temperature, the white precipitate was separated by high-speed centrifugation at 3000 rpm for 15 min, washed with ethanol and ultra-pure water for several times to remove impurities, and then dried in

vacuum at 60°C for 24 h and heat at 550°C for 3 h. In order to investigate the effect of temperature on the morphology of TiO₂, the synthesized products were calcinated at different temperatures (350, 550, 700 and 1000°C) for 3 h, respectively.

Immobilization of Synthesized TiO₂ on the Surface of Stainless Mesh

The stainless steel mesh was firstly cleaned with acetone, ethanol and pure water under ultrasonic conditions for 1 h, and then dried at 100°C for 30 min. In typical coating procedure, 0.1 g of synthesized TiO₂ and 10 mL DMSO were mixed in a glass under ultrasonication for 2 h. Then after, the mesh was immersed into the suspension by using a dip-coat method (immersion rate: 400 mm/min; immersion time: 5 s and withdrawal rate: 100 mm/ min). Then, the mesh was removed, dried at 60°C for 1 h and calcinated at 450°C for 3 h.

Characterization

The phase structure and phase purity of the synthesized products were examined by X-ray diffraction (XRD), using a Rigaku D/max 2550VB/PC diffractometer with Cu K α ($\lambda=0.154$ nm) radiation as the incident beam. The morphology and the chemical composition of substrates were observed by a scanning electron microscope equipped with energy dispersive spectrometry (SEM-EDS, JSM-6360LV, Japan). The static contact angles of water/oil droplets in the air and in the water were measured with 5 μ L droplet using a Kruss DSA 100 (Kruss Company, Ltd., Germany) at ambient temperature. In the air environment, the static contact angle measurements of oil droplets were conducted by using leybonol and olive oil while the underwater measurements were evaluated with leybonol, olive oil, and petroleum ether. In the air, oil droplets were directly deposited on the mesh using a micro-syringe, while for the underwater contact angle measurement, the mesh was first immersed in water and oil droplet was carefully deposited on its surface using a micro-syringe. Photograph in Figure was obtained on a camera (Nikon D5300). Due to the unavailability for appropriated mechanical analysis, the oil and water separation process was conducted using leybonol in order to investigate the recyclability of TiO₂ coated mesh. The mesh with a size of 2 \times 2 cm² was fixed on a glass tube (diameter 1.5 cm) and pre-wetted by water, and then a mixture of oil and water (1:1, v:v) was poured into the tube. After the separation test, the mesh was removed, cleaned with ethanol and pure water, and then dried at 100°C for 1 h. The oil/water separation efficiency of the mesh was estimated according to $\hat{A}=(m_1/m_0) \times 100$, where m_0 and m_1 were the mass of the oil before and after the separation process, respectively. The average values were obtained by repeating the measurement five times and during the whole study, the pH was not investigated.

RESULTS AND DISCUSSION

X-ray Diffraction of Synthesized TiO₂

The X-ray patterns of the synthesized TiO₂ are displayed in Figure 1. In all cases, the as-synthesized products exhibited a relatively strong diffraction peak, characterizing their crystallinity. The diffraction peaks of synthesized products calcinated at temperature varying from 350 to 700°C appearing at 2 θ of 25.3°, 37.8°, 48.1°, 55.1°, 62.7°, 70.3° and 75.1° (line a to c) could be indexed to the anatase phase (JCPDS No. 21-1272), indicating that the synthesized product was pure anatase TiO₂ [10,32]. However, diffraction peaks observed at 2 θ of 27.5°, 39.2°, 41.2°, 44.1°, 56.6°, 65.5° for the product calcinated at 1000°C are identified for rutile phase (JCPDS No. 21-1276) [33].

From the above observations, we can notice that the synthesized products calcinated at temperatures below 700°C are in TiO₂ anatase phase, and a further increase in calcination temperature leads to a mixture of anatase and rutile phases. In addition, as the peak intensities increase as increasing calcination temperature, the product calcinated at elevated temperature may be in high crystallinity.

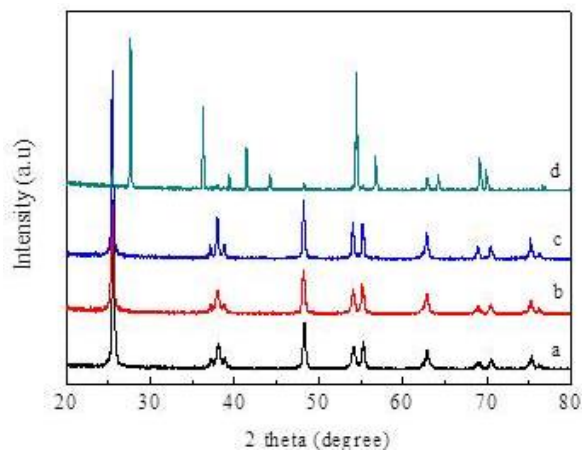


Figure 1. XRD patterns of calcined TiO₂ at (a) 350°C, (b) 550°C, (c) 700°C and (d) 1000°C

SEM Images and EDS Analysis of Synthesized TiO₂

The morphology of the synthesized TiO₂ was studied by using SEM, and the results are displayed in Figure 2a-2c. It can be observed that the synthesized TiO₂ consisted of well-defined sheet-shaped structures having a rectangular outline with diameters varying from 34 to 67 nm. The nano-sheets keep in good sheet structure when the calcination temperature increased up to 700°C. Further increasing of the calcination temperature conducted in an increase of diameters of the nano-sheets forming an agglomeration.

The spectrum of electron dispersive spectroscopy of the calcinated product at 450°C is illustrated in Figure 2d. The peak of Ti appeared at around 0.2 keV and another intense peak at 4.5 keV, O displayed a peak at around 0.2 keV.

The results of SEM and EDS analysis are conformed to that of XRD analysis and suggested that the morphology and microstructure of synthesized products varied over the calcination temperature [33,34].

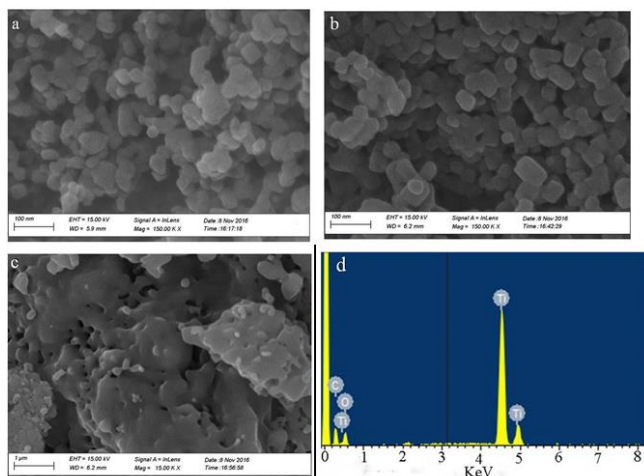


Figure 2. SEM images of calcined TiO₂ at (a) 350°C, (b) 500°C, (c) 1000°C and (d) EDS spectrum of calcined TiO₂ at 550°C

Contact Angle Measurement

The wettability through water and oil of the mesh was evaluated by measuring the contact angle in the air and underwater environments. From Figure 3a, it is indicated that unmodified mesh exhibited an oleophilic/hydrophobic behavior with the oil contact angle (Oca) of 45.4° and 31.9° for leybonol and olive oil respectively; the water contact angle (Wca) of 105.4°. After immobilization of synthesized TiO₂ nano-sheets, the surface of the modified mesh exhibited a relative strong oil repelling behavior that is characterized by the increase of Oca through leybonol and olive oil (109.3° and 98.3°); while the Wca of 4.6°. The underwater contact angle measurements were conducted using leybonol, olive oil and petroleum ether. It can be clearly seen in Figure 3b that all Oca over the surface of modified mesh were larger than 150° and it is important to note that leybonol and petroleum ether were supported by a needle as their droplets did not adhere to the surface.

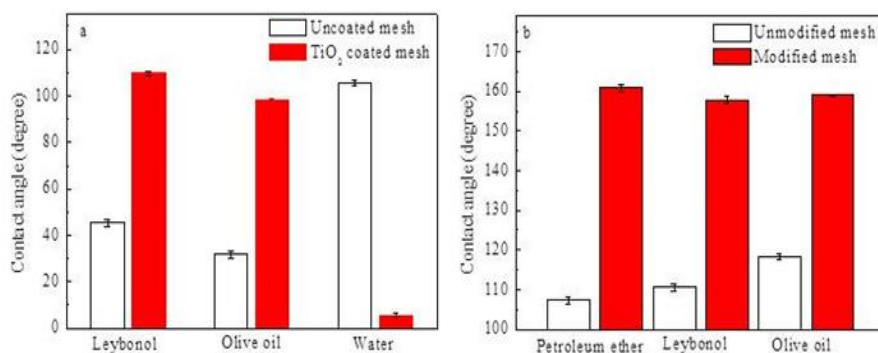


Figure 3. Contact angle measurement of oil and water droplets in (a) air and (b) in water environments

Above observations suggest that the modification of wettability of the mesh is largely attributed to the presence of the Synthesized TiO₂ immobilized on its surface. As it is well known, TiO₂ is naturally hydrophilic due to the presence of hydroxyl group (OH-) on its surface [18,35,36]. When TiO₂ is immobilized on the surface of the membrane, it will increase the hydrophilicity behavior of the membrane by generating hydroxyl radical (•OH) [37,38]. Moreover, the underwater superoleophobicity of the modified mesh can be easily explained by Cassie-Baxter analysis. It is said that the hydrophilic surface in the air generally becomes oleophobic underwater due to the lower surface tension of oil compared to that of water [39-41]. So the trapped water molecules at the interface between the oil droplet and the surface repelled oil molecules.

The modified mesh was further involved in the separation process of leybonol/water and olive oil/water mixtures. Figure 4a is the photographs of the oil/water separation device. It was observed that water easily permeated through the mesh and dropped into the beaker below, while oil was retained above the mesh even for a long time. It is interesting to observe that gravity separation method was used in this study and no external force was used. The results from Figure 4b revealed that the separation efficiency of the modified mesh was calculated up to 95% leybonol/water and olive oil/water mixtures. In addition, the modified coated mesh retains excellent superoleophobic behavior after thirty cycles of use with the separation efficiency above 90%, suggesting good recyclability of TiO₂ coated mesh.

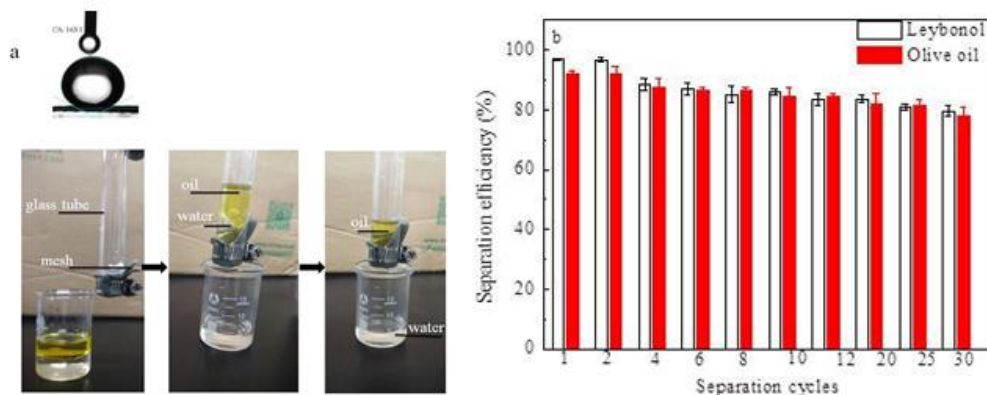


Figure 4. (a) Photographs of olive oil/water separation device using TiO_2 coated mesh and (b) Leybonol/water and olive oil/water separation efficient in 30 cycles reuse using TiO_2 coated mesh

X-ray Diffraction, SEM Images and EDS Analysis of the Modified Mesh

In order to investigate the presence of TiO_2 , the modified mesh was further characterized by XRD, SEM, and EDS analysis. SEM image of the unmodified mesh is depicted in Figure 5a. It is clearly shown that the mesh exhibited a smooth surface with the pore size of 75 microns as showed in. After immobilization, Figure 5b revealed that the TiO_2 coated mesh was covered by a uniformity thin layer of TiO_2 nano-sheets.

Figure 5c displayed the XRD patterns of unmodified and modified mesh along synthesized TiO_2 nano-sheets. As it is displayed in line a and line b, the main diffraction patterns of both unmodified and modified mesh appeared at 2θ of 43.8° could be indexed to the stainless steel (JCPDS No. 33-0945) and no other peaks cannot be observed, that is might be due to the low content of TiO_2 nano-sheets and its high dispersion degree on the surface of the mesh.

The chemical compositions of the meshes were investigated by energy dispersive spectrometry and the result is presented in Figure 5d. It can be observed that the modified mesh is composed of O, Fe, Cr, and Ti elements, indicating the presence of Ti element on the surface of the I mesh.

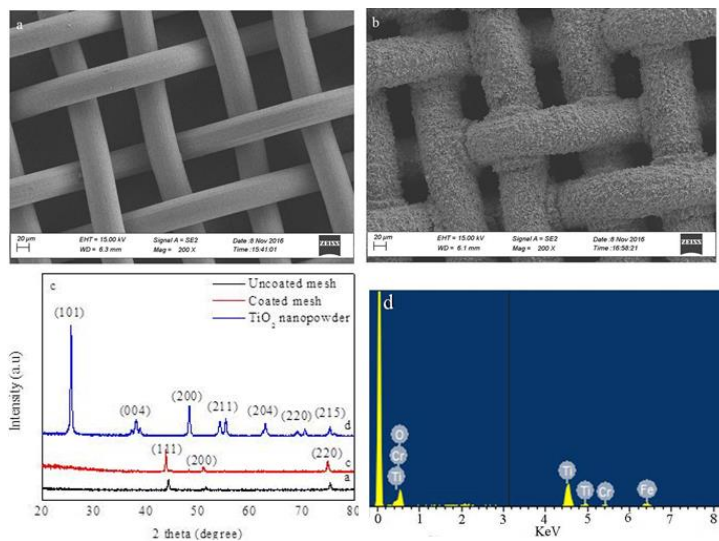


Figure 5. (a) XRD patterns of unmodified and modified mesh and synthesized TiO_2 nano-sheets. SEM images of (b) unmodified mesh, (c) modified mesh and (d) EDS spectrum of modified mesh

Above analysis suggested that the thin coated film might provide excellent separation performance of the mesh. Surface pore sizes remarkably affect the wettability of the surface for smaller is the diameter size of the membrane, higher is hydrophilic of the surface. In this study, the TiO₂ nano-sheets did not obstruct the pore of the mesh as shown in SEM images. In addition, it is well known that high crystallinity and surface roughness are crucial to obtaining hydrophilicity and that is occurred by annealing at high temperature. That analysis is supported by Wenzel statement stating that for an initially hydrophilic surface, the increasing roughness led to an increase in the hydrophilicity [14,42]. In the present study, the drying temperature is a benefit to enhance the wettability of the mesh as it might provide the generation of the hydroxyl group (OH⁻) and achieving an underwater superoleophobic surface that has many advantages in the removal of oil in oil/water emulsion.

CONCLUSION

TiO₂, synthesized by using the hydrothermal method and calcined at different temperatures was successfully immobilized on the surface of the commercial stainless mesh by dip coating process. The characterization results revealed that synthesized TiO₂ was in anatase phase with a sheet-shaped structure having a rectangular outline and diameters varying from 34 to 67 nm. Moreover, the calcination temperature can modify the crystalline phase of the product as the mixed phase of rutile and anatase was obtained at 1000°C. The immobilization of the synthesized TiO₂ remarkably affected the wettability behavior of the surface of the mesh from oleophilic to underwater superoleophobic with the underwater oil contact angles larger than 150°. Moreover, modified mesh exhibited good oil/water separation efficiency up to 90% even after thirty cycles of reuse. Further characterization results of the modified mesh revealed that the TiO₂ nanosheets were uniformly dispersed and made a thin separating layer on the surface of the mesh. The results of this study suggest a simple and economical method to prepare underwater superhydrophilic/superoleophobic surface and indicate that additional studies could be conducted for widespread industrial application of the synthesized TiO₂ in membrane coating technology.

ACKNOWLEDGMENTS

This study was supported by the Innovation Platform for the Development and Construction of Special Project of Key Laboratory of Tibetan Medicine Research of Qinghai Province (No. 2017-ZJ-Y11), Qinghai Provincial Science Foundation (2017-SF-A8), Yulin Municipal Science and Technology Bureau Science Foundation and China post-doctorate program at Chang' An University.

REFERENCES

- [1] A Fujishima; K Honda. *Nature*. **1972**, 238, 37.
- [2] A Kitada; G Hasegawa; Y Kobayashi; K Kanamori; K Nakanishi; H Kageyama. *J Am Chem Soc*. **2012**, 134(26), 10894-10898.
- [3] F Yang; Y Liu; J Ye; G Wang; W He. *Mater Lett*. **2018**, 233, 28-30.
- [4] Q You; G Ran; C Wang; Y Zhao; Q Song. *J Coat Technol Res*. **2018**, 15(5), 1013-1023.
- [5] E Pelizzetti; V Maurino; C Minero; V Carlin; MTosato L; E Pramauro; O Zerbinati. *Environ Sci Technol*. **1990**, 24(10), 1559-1565.
- [6] L Biyoghe Bi Ndong; MP Ibondou; Z Miao; X Gu; S Lu; Z Qiu; Q Sui; Mbadinga SM. *J Environ Sci*. **2014**, 26(5), 1188-1194.
- [7] Y Yu; J Miao; J Wang; C He; J Chen. *Catal Sci Technol*. **2017**, 7(7), 1590-1601.
- [8] N Serpone; P Maruthamuthu; P Pichat; E Pelizzetti; H Hidaka. *J Photochem Photobiol A Chem*. **1995**, 85(3), 247-255.
- [9] B Bai; N Quici; Z Li; Puma GL. *Chem Eng J*. **2011**, 170(2), 451-456.

- [10] M Ye; Z Chen; W Wang; J Shen; J Ma. *J Hazard Mater.* **2010**, 184(1-3), 612-9.
- [11] S Yuan; C Chen; A Raza; R Song; TJ Zhang; SO Pehkonen; B Liang. *Chem Eng J.* **2017**, 328, 497-510.
- [12] AE Livari; A Aroujalian; A Raisi. *Procedia Eng.* **2012**, 44, 1783-1785.
- [13] N Misdan; AF Ismail; N Hilal. *Desalination.* **2016**, 380, 105-111.
- [14] L Zhang; Y Zhong; D Cha; P Wang. *Sci Rep.* **2013**, 3, 2326.
- [15] WJ Lau; AF Ismail; N Misdan; Kassim MA. *Desalination.* **2012**, 287, 190-199.
- [16] C Zhou; Y Li; H Li; X Zeng; P Pi; X Wen; S Xu; J Cheng. *Surf Coat Technol.* **2017**, 313, 55-62.
- [17] V Moghimifar; A Raisi; A Aroujalian. *J Memb Sci.* **2014**, 461 69-80.
- [18] J Jeevahan; M Chandrasekaran; Britto G Joseph; RB Durairaj; G Mageshwaran. *J Coat Technol Res.* **2018**, 15(2), 231-250.
- [19] H Gao; P Sun; Y Zhang; X Zeng; D Wang; Y Zhang; W Wang; J Wu. *Surf Coat Technol.* **2018**, 339 147-154.
- [20] J Chen; D Guo; C Huang; X Wen; S Xu; J Cheng; P Pi. *Mater Lett.* **2018**, 233, 328-331.
- [21] J Wang; Y Zheng. *Sep Purif Technol.* **2015**, 181, 183-191.
- [22] M Padaki; R Surya Murali; MS Abdullah; N Misdan; A Moslehyani; MA Kassim; N Hilal; Ismail AF. *Desalination.* **2015**, 357, 197-207.
- [23] Z Chen; C Zhou; J Lin; Z Zhu; J Feng; L Fang; Cheng J., *J Sol-Gel Sci Technol.* **2017**, 85(1), 23-30.
- [24] L Gelde; A Cuevas; M Martínez de Yuso; J Benavente; V Vega; A González; V Prida; B Hernando. *Coatings.* **2018**, 8(2), 60.
- [25] E Karimi; A Raisi; A Aroujalian. *Polymer.* **2016**, 99, 642-653.
- [26] J Kim; Van der B Bruggen. *Environ Pollut.* **2010**, 158(7), 2335-2349.
- [27] L Zhang; J Gu; L Song; L Chen; Y Huang; J Zhang; T Chen. *J Mater Chem A Mater.* **2016**, 4(28) 10810-10815.
- [28] J Yu; J Shi; S Yu. *J Sol-Gel Sci Technol.* **2017**, 84(2) 239-245.
- [29] Y Li; Y Liu; C Liu; C Li; H Li. *Mater Lett.* **2018**, 233 16-19.
- [30] A Razmjou; A Resosudarmo; RL Holmes; H Li; J Mansouri; V Chen. *Desalination.* **2012**, 287, 271-280.
- [31] L Biyoghe Bi Ndong; X Gu; S Lu; Ibondou MP; Z Qiu; Q Sui; SM Mbadinga; B Mu. *Chem Eng Sci.* **2015**, 123, 367-375.
- [32] Biyoghe Bi L Ndong; MP Ibondou; X Gu; M Xu; S Lu; Z Qiu; Q Sui; Mbadinga SM. *Water Air Soil Pollut.* **2014**, 225(5).
- [33] HL Shen; HH Hu; DY Liang; HL Meng; PG Li; WH Tang; C Cui. *J Alloy Compd.* **2012**, 542 32-36.
- [34] Y Yu; J Wang; Parr JF. *Procedia Eng.* **2012**, 27 448-456.
- [35] C Gao; Z Sun; K Li; Y Chen; Y Cao; S Zhang; L Feng. *Energy Environ Sci.* **2013**, 6(4) 1147.
- [36] J Li; L Yan; W Hu; D Li; F Zha; Z Lei. *Colloids Surf A.* **2016**, 489, 441-446.
- [37] MA Gondal; MS Sadullah; MA Dastageer; GH McKinley; D Panchanathan; Varanasi KK. *ACS Appl Mater Interfaces.* **2014**, 6(16) 13422-13429.
- [38] S Leong; A Razmjou; K Wang; K Hapgood; X Zhang; H Wang. *J Memb Sci.* **2014**, 472, 167-184.
- [39] S Nishimoto; M Ota; Y Kameshima; M Miyake. *Colloids Surf A.* **2015**, 464, 33-40.
- [40] H Liu; A Raza; A Aili; J Lu; A AlGhaferi; T Zhang. *Sci Rep.* **2016**, 6, 25414.
- [41] X Liu; P Hou; X Zhao; X Ma; B Hou. *J Coat Technol Res.* **2018**, 16(1), 71-80.
- [42] J Liu; P Li; L Chen; Y Feng; W He; X Yan; X Lü. *Surf Coat Technol.* **2016**; 307, 171-176.